Adaptive Vector Control of Grid-tied VSC using Multilayer Perceptron-Recurrent Neural Network

Prabhat Ranjan Bana
Department of Electric Power Engineering
Norwegian University of Science and Technology
Trondheim, Norway
Email: prabhat.r.bana@ntnu.no

Mohammad Amin
Department of Electric Power Engineering
Norwegian University of Science and Technology
Trondheim, Norway
Email: mohammad.amin@ntnu.no

***Abstract*—The standard vector control is widely used for grid-connected voltage source converters (VSCs), however, the inability to satisfactorily operate at the desired level under different dynamic scenarios and grid conditions limit its application. This paper presents an artificial neural network (ANN) based vector control for the grid-connected VSCs. The Multilayer Perceptron-Recurrent Neural Network (MP-RNN) approach is used in this work which generates the reference current for the current controller of the VSC. To verify the effectiveness of the proposed control, the MP-RNN-based vector control is implemented for a grid-connected VSC in the MATLAB/Simulink environment and the MP-RNN structure is trained by the Levenberg-Marquardt based backpropagation algorithm. Simulation results are presented and compared with the vector control with and without the proposed ANN-aided control. The results clearly show that the proposed control has a better dynamic performance in damping the oscillation introduced by the dc-link dynamics of the VSC. Further, the dynamic performance of the proposed control has been verified with a model implemented in the OPAL-RT environment considering different dynamic test cases.**

***Index Terms*—Artificial neural network (ANN), Multilayer Perceptron-Recurrent Neural Network (MP-RNN), Damping, Voltage oscillation, Voltage source inverter (VSC)**

I. Introduction

Power electronics converters are the enabling technology for integrating renewable energy sources (RES) such as solar PV, wind energy as well as the battery storage, electric vehicles, highly dynamic power electronics loads into the utility grid. The effective application of this technology depends on the appropriate modeling and analysis, control design successful implementation of the control algorithm of the converters [1], [2]. The use of a voltage source converter (VSC) in parallel with the grid employing a closed-loop control strategy to address different challenges such as damping the high voltage oscillations, suppressing the harmonic pollution have been the key research aspect over the last decade [3], [4]. Nevertheless, the traditional current-controlled inverters are inherently incompatible with the grid as it fails to track the accurate reference signal under sudden disturbance/dynamic conditions [5]. In addition, when RES units are employed for the medium/high voltage application or integrated with the distribution sector, the presence of the LC-resonances in the system make the damping system further weak and produces unwanted oscillations, over-voltage, and even instability due to the improper interaction between the power electronics converter and its control system [6], [7].

In the recent past, different control approaches are developed in the literature to address the aforesaid concerns. For example, an active damping control approach is adopted in [6] to address the low-frequency oscillatory phenomena in a grid-connected wind farm system. In [8] an enhanced higher-order generalized integrator control is proposed to extract optimum quality power from the PV system while the grid is weak. Further, iterative mathematical approach and artificial intelligence (AI) algorithms are gaining more attention to compute the best value by solving the non-linear transcendental equations of the power electronics system. The least mean square (LMS) method involves the simplest mathematical equations [9] and works iteratively to estimate the reference signal, but eventually turns unstable under the weak grid and low signal to noise ratio conditions. To tackle this issue, the least mean fourth (LMF) method is introduced in [10] for the said application in compromise with the complexity.

Genetic algorithm (GA) is one kind of AI algorithm, that is based on evolutionary biology and is widely employed for power electronics application, but with an essential trade-off between computation time and accuracy [11]. Fuzzy logic has proven its faster convergence rate in approaching a solution when information about the accurate/actual signal is unknown and therefore can be considered as a suitable AI technique to control unstable RES units like solar and wind, where the solar insolation and wind velocity level are anonymous [12]. In [13], fuzzy logic strategy is employed to form an adaptive PI-control loop for dc-link voltage regulation in a grid-tied PV system. The particle swarm optimization (PSO) algorithm is inspired by the food searching behavior of the swarms and is majorly utilized to extract the maximum power from the RES units and to tune the PI-parameters of the current controller [14]. The performance of the PSO is mainly influenced by the way it updates its position and velocity from the past recorded values. Amidst all AI techniques, Artificial Neural Network (ANN) is a powerful and modern AI technology that is extensively investigated for different applications [12]. ANN algorithm is implemented in [15] to reconstruct the glitched signals obtained from the standard current controller for a single-phase grid integrated solar PV system to ensure system performance

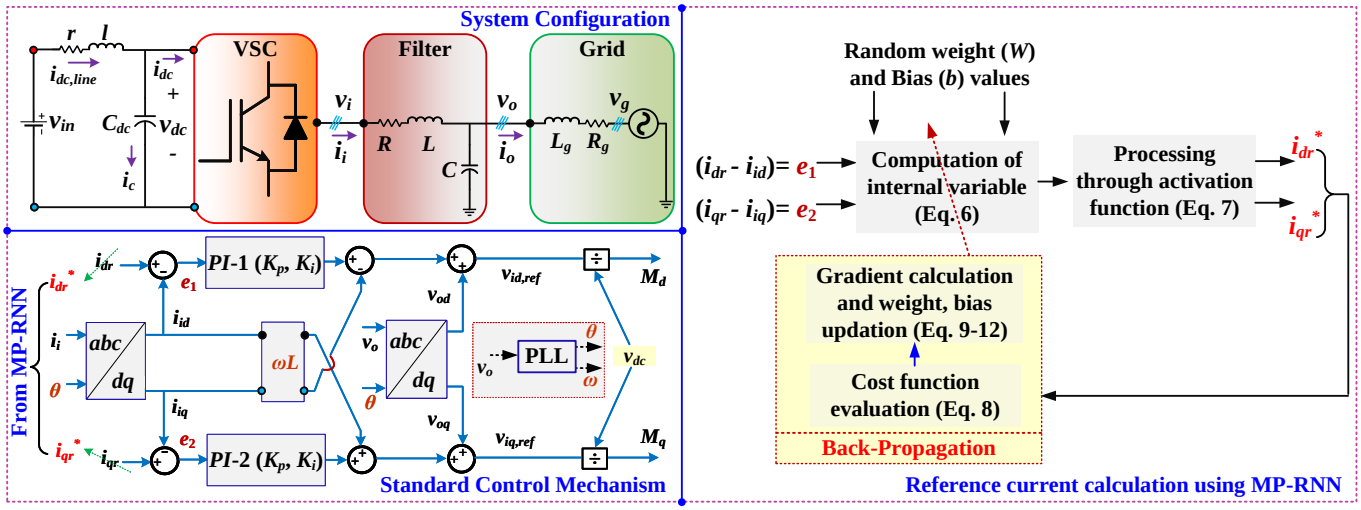

Fig. 1. Grid-tied VSC system with MP-RNN aided current control architecture

and reliability. In [4], single layer ANN is employed to extract the three-phase abc-components for the power factor improvement of grid-connected VSC system, but with the cost of increased control complexity. Authors in [16] have utilized the ANN algorithm for generating voltage reference signal to maintain the dc-link voltage at the desired level, which is further trained by the artificial bee colony algorithm to achieve better performance under different disturbances.

With further improvement in the current control strategies, this work proposes a Multilayer Perceptron-Recurrent Neural Network (MP-RNN) algorithm-based current controller, which is adaptive to the external disturbances as well as damps-out the high voltage oscillations of the system without hampering the grid-voltage shape. The generalized working structure and control algorithm of ANN to generate the accurate current reference signals for the current control loop of VSC is delineated in the next section followed by the training of process of MP-RNN using the Levenberg-Marquardt (LM) backpropagation algorithm. In the end, comparative simulation results of the vector control with and without the proposed ANN-aided control are provided considering a large and continuous disturbance in the reference signal. Also, the real-time applicability of the proposed control is validated in the OPAL-RT environment considering the similar dynamic test case.

II. Modeling of The System

The schematic of the grid-connected VSC system with the current control loop is shown in Fig. 1. The circuitry of the system has three main components, which are a three-phase distribution grid, filter circuit, and VSC. This work includes the use of a three-leg average VSC model. All the AC side parameters are converted into the dq-domain of a synchronous reference frame (SRF) by utilizing the park transformation matrix. In this context, the VSC model dynamics in p.u. system can be expressed as in (1-3) by considering ω_b as the angular grid frequency which acts as the base of the system and ω_g is the p.u. grid frequency [6].

$$\frac{di_{id}}{dt} = \frac{\omega_b}{L}v_{id} - \frac{\omega_b}{L}v_{od} - \frac{\omega_b R}{L}i_{id} + \omega_b\omega_g i_{iq} \tag{1}$$

$$\frac{di_{iq}}{dt} = \frac{\omega_b}{L}v_{iq} - \frac{\omega_b}{L}v_{oq} - \omega_b\omega_g i_{id} - \frac{\omega_b R}{L}i_{iq} \tag{2}$$

$$\frac{dv_{dc}}{dt} = \frac{\omega_b}{C_{dc}}i_{dc,line} - \frac{\omega_b\left(i_{id}v_{id} + i_{iq}v_{iq}\right)}{C_{dc}v_{dc}} \tag{3}$$

Moreover, the current controller loop generates the voltage reference signals ($v_{id,ref}$ & $v_{iq,ref}$) for the switching pulse generation stage which is mathematically represented in (4 & 5).

$$v_{id,ref} = (i_{dr} - i_{id})\left(K_p + \frac{K_i}{S}\right) + v_{od} - \omega L i_{iq} \tag{4}$$

$$v_{iq,ref} = (i_{qr} - i_{iq})\left(K_p + \frac{K_i}{S}\right) + v_{oq} + \omega L i_{id} \tag{5}$$

where, i_{dr} & i_{qr} are the dq-axis reference currents, K_p & K_i are PI-controller gains, and ω is the p.u. frequency obtained from phase locked loop (PLL).

III. MP-RNN Formation for Proposed Application

A. Working of MP-RNN

ANN is a pattern recognition concept inspired by the way the human brain works. It provides the best global solutions, where there is no direct mathematical relationship between input-output. In the MP-RNN structure shown in Fig. 2, e_1 and e_2 are fed to the input layer of the ANN. Afterward, the input layer is connected to the hidden layer via a set of weights (W_1). Six nodes are considered in the hidden layer for this problem, and each node is connected to the nodes of the output layer via another set of weights (W_2), in the same way, the

previous layer is connected. Apart from the weight matrices, each node (except the input layer) is assigned with a variable known as bias factor b. Finally, the outputs of the ANN can be collected at the output layer. It is worth mentioning, the adopted ANN structure is the MP-RNN, which accepts the sequential time-series data as input.

$$u_{k(i,j)} = W_{k(i,j)} e_i + b_{k(j)} \tag{6}$$

$$F\left[W_{k(i,j)}, b_{k(j)}\right] = \frac{1 - e^{-2u_{k(i,j)}}}{1 + e^{-2u_{k(i,j)}}} \tag{7}$$

$$C_f = \sum_{n=1}^{N} \left\{ \left[i_{dr}^* - i_{id}\left(n\right)\right]^2 + \left[i_{qr}^* - i_{iq}\left(n\right)\right]^2 \right\} \tag{8}$$

Forward propagation is the default method with which the ANN tries to find the output by considering the input variables, weight, and bias matrices. At the beginning of this process, the weight matrices can be initialized randomly. Once the ANN receives the input variable (e_i), it will multiply them with the weight matrix, $W_{k(i,j)}$ (for the k^{th} layer, i^{th} input, and j^{th} node) followed by the addition with bias factor, $b_{k(j)}$ to obtain the internal variable 'u' of the hidden layer as given in (6). The internal variable is then processed through an activation function presented in (7), and the output of the activation function acts as an input to the output layer which again goes through the above process to compute the final output of ANN. However, the internal method of the ANN alone is not sufficient enough to determine the optimum solution under distorted conditions, and therefore, the MP-RNN structure must be trained again. Searching for the best possible values of weight and bias matrices in order to match the reference current components with actual current as close as possible is called training of the ANN. Levenberg-Marquardt based backpropagation algorithm (LMBA) is widely used to train the ANN [15] whose goal is to continuously evaluate the gradient of the cost function (C_f) as given in (8) w.r.t weight and bias factor to find their new value. The weight adaptation to the new value follows the procedure given in (9 & 11) and in a similar fashion, the bias factor can also be updated.

$$\frac{dC_f}{dW} = \frac{d\sum_{n=1}^{N}\left[C\left(n\right)\right]^2}{dW} = \sum_{n=1}^{N} 2C\left(n\right)\frac{dC\left(n\right)}{dW} = 2Cj\left(W\right)^T \tag{9}$$

$$C\left(n\right) = \left[i_{dr}^* - i_{id}\left(n\right)\right]^2 + \left[i_{qr}^* - i_{iq}\left(n\right)\right]^2 \tag{10}$$

$$W_{update} = W + \Delta W \tag{11}$$

$$\Delta W = -\left[j\left(W\right)^T * j\left(W\right) + \mu I\right]^{-1} j\left(W\right)^T C \tag{12}$$

where C is the summed termed of $C(n)$, j is the jacobian matrix [15]

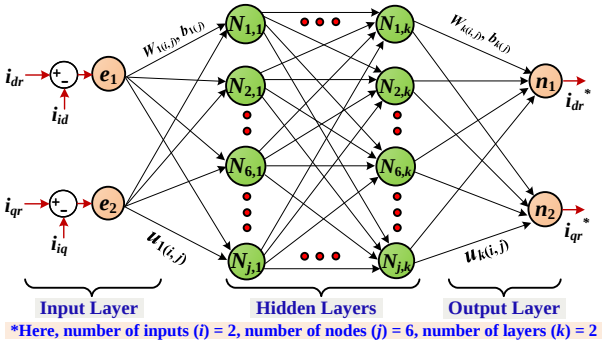

Fig. 2. Generalised structure of proposed MP-RNN

B. Training of MP-RNN

Once the MP-RNN structure is formed by considering the above-discussed constraints, it has to be trained off-line before it is utilized for any application. In the present work, the errors (e_1 & e_2) are given as input to the illustrated MP-RNN structure in Fig. 2, whose target is to generate the new reference signals so that the steady-state errors caused by the PI-controller can be removed. Several samples of input values can be stored in a look-up table considering different disturbances in the reference signal under weak-grid conditions and similarly the target value can also be stored in another lookup table. Afterward, these samples can be processed for the training process. The LMBA method follows the following Pseudo-code for the successful training of MP-RNN.

- *Step*-1: Initialize the training process by setting the $epoch$ value as 1
- *Step*-2: Initialize all the training parameters $\mu, \mu_{max}, epoch_{max}$ and minimum value of the gradient of the cost function as defined in the equation (9)
- *Step*-3: The weight matrix can be initialized with random values in the range $[0, 1]$
- *Step*-4: Evaluate the cost function (C_f) given in (8) and Jacobian matrix (j)
- *Step*-5: Compute (9) for the updated C_f value and check whether it exceeds the minimum defined value. If the status is yes then update the weight value using (11 & 12) else stop training as the minimum gradient is reached.
- *Step*-6: In addition to step-5, adjust the learning rate value (μ) in the decreasing direction of C_f
- *Step*-7: The complete training process follows three stopping criterias. Stop the training process if, (a) μ defined in $step$-2 reached its maximum defined value (μ_{max}), (b) Maximum $epoch$ value is reached, (c) minimum gradient value given in expression (9) is satisfied with its predefined value initialized in $step$-2

Afterward, the MP-RNN structure can be deployed for the defined objective in the grid-tied VSC system shown in Fig. 1. Now, for any input disturbances, the trained MP-RNN structure has learned the ability to eliminate almost all possible errors before it is fed to the PI-control loop.

TABLE I
ANN CONTROLLER PARAMETERS

Parameter	Value	Parameter	Value	Parameter	Value
Input neurons (i)	2	Output neurons (o)	2	Minimum gradient value of C_f	10^{-10}
Hidden neurons (j)	6	μ_{max}	10^{10}	K_p, K_i	1.27, 14.25
number of layers (k)	2	$epoch_{max}$	1000	Sampling time (T_s)	100 μs

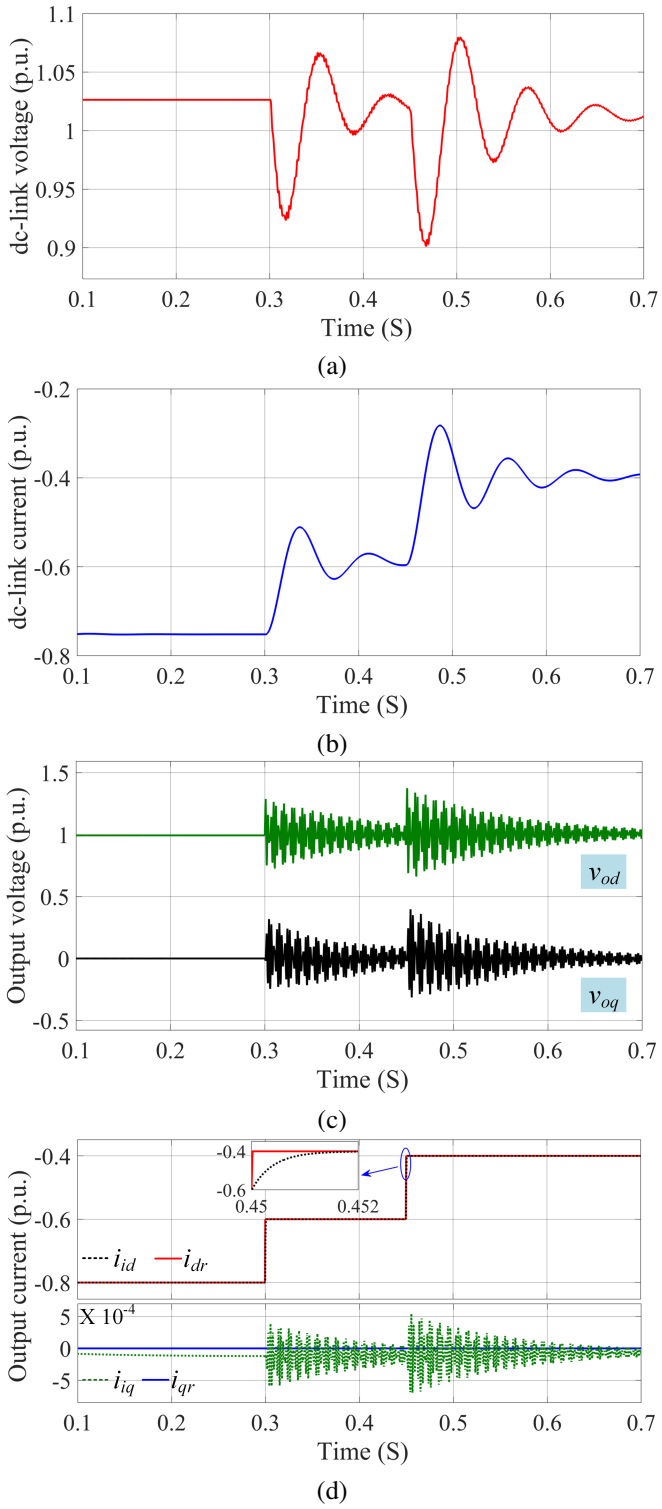

Fig. 3. Simulation results with standard control with change in i_{dr} by 0.2 p.u., at 0.3, & 0.45 S (a) v_{dc}, (b) i_{dc}, (c) v_o, (d) i_i

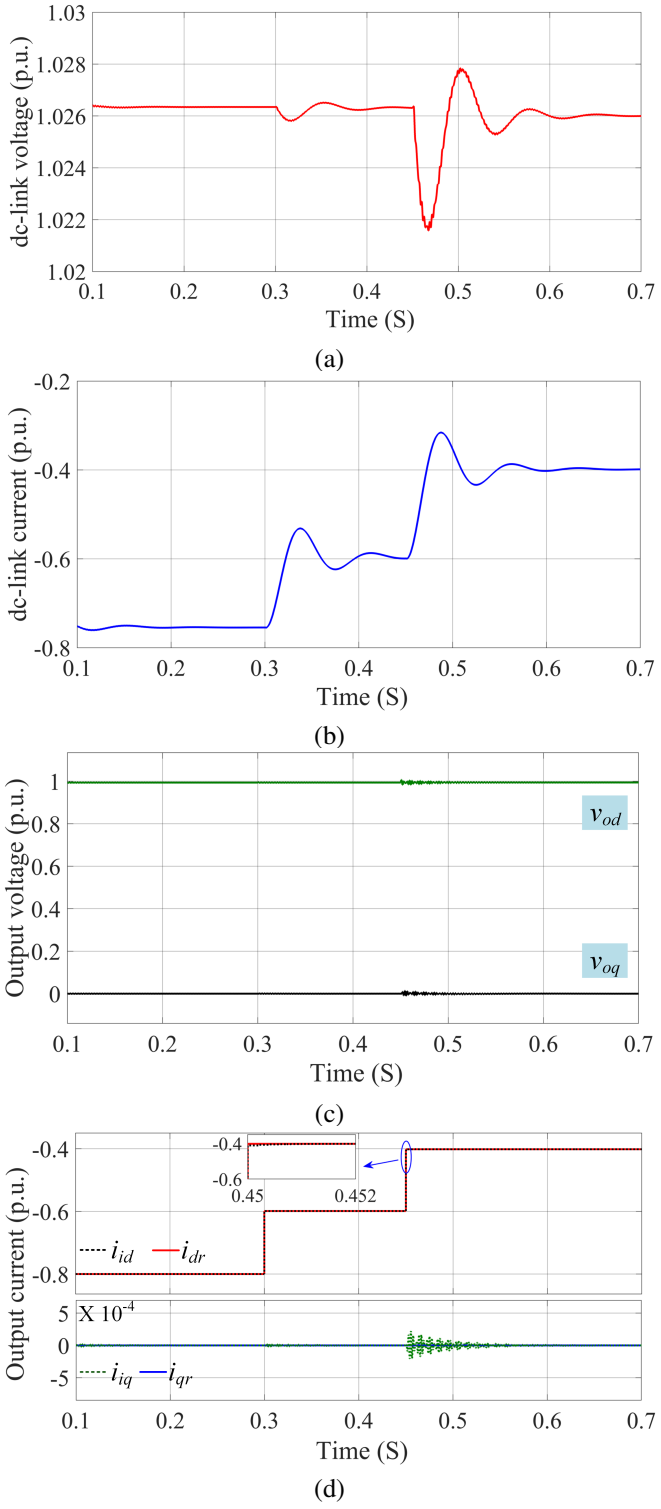

Fig. 4. Simulation results with proposed control with change in i_{dr} by 0.2 p.u., at 0.3, & 0.45 S (a) v_{dc}, (b) i_{dc}, (c) v_o, (d) i_i

IV. Performance Evaluation

A three-phase grid-tied p.u. system in integration with an average VSC model as shown in Fig. 1 is developed in the MATLAB/Simulink environment as well as in a real-time simulation platform (OPAL-RT). Both standard closed-loop control and ANN-based adaptive controls are implemented to study the system performance under dynamic scenarios in consideration of the parameters presented in Table I & II.

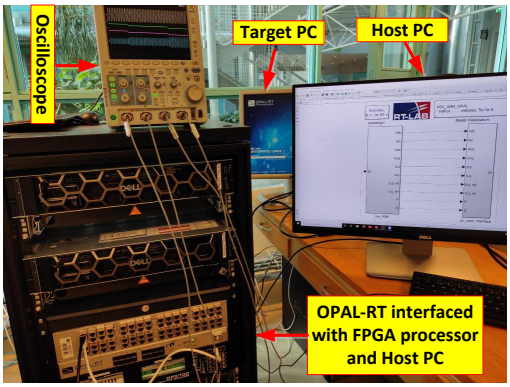

Fig. 5. OPAL-RT setup for real-time operation

A. Simulation Results

In reference to the standard controller and ANN application stated in the previous section, the parameters of the PI-controllers employed in the current control loop is firstly tuned for the best value by modulus optimum method (here K_p = 1.27, K_i = 14.25), then after ANN with two inputs and two outputs is trained with the same control parameters. It should be noted, same PI-gains are considered for both the controllers during performance evaluation. Moreover, all the simulation results are produced when the d-axis reference current magnitude is suddenly reduced by 0. 2 p.u. at 0.3 and 0.45 sec. In this context, the output findings using the standard control are presented in Fig. 3, where the dc-link voltage (v_{dc}) is poorly damped and becomes highly unstable with the sudden change in reference current, also dc-current (i_{dc}) takes a longer time to get settled at the new steady-state value. Further, the oscillation gets propagated to the output voltage (v_o) which can be observed in Fig. 3(c), this is all because the actual current takes a certain time to track the reference value which can be visualized from Fig. 3(d). On the other hand, results obtained using the proposed control are shown in Fig. 4, where the damping response is very smooth, *i.e.*, the magnitude of the oscillations of the dc-voltage and current are less. Also, it attains the steady-state value quickly (within 10 cycles). It is noteworthy that, PCC voltage components are less influenced by the change in d-axis reference current as indicated in Fig. 4(c), which evaluates the effectiveness of the ANN-based control approach. The effective tracking performance of the proposed control can also be verified from Fig. 4(d).

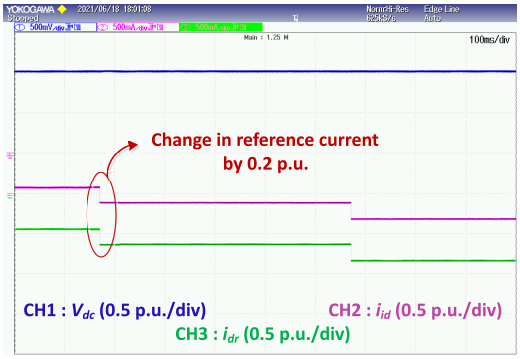

(a)

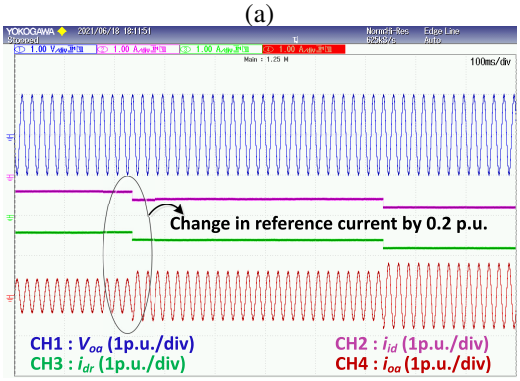

(b)

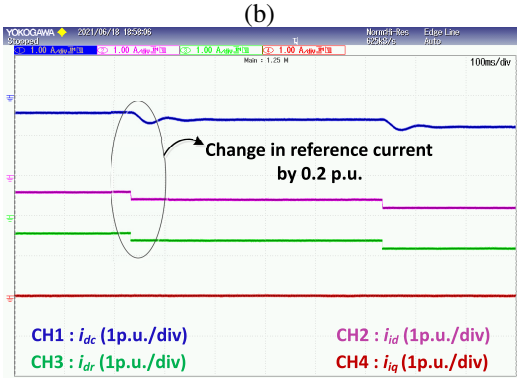

(c)

Fig. 6. Results obtained from OPAL-RT platform, captured with YOKOGAWA scope-coder (a) v_{dc}, i_{id}, and i_{dr}, (b) i_{dc}, i_{id}, i_{dr}, and i_{iq}(c) v_{oa} (a-axis), i_{ia} (a-axis), i_{id}, and i_{dr}

B. Real-time Simulation Analysis

Performance evaluation of any advanced control techniques in a real-time simulation environment is the first step before deploying the same for the real/practical usage in any industry sector. In this perspective, the proposed ANN-based current controller and the grid-connected VSC system are both modeled in the OPAL-RT environment. The complete setup picture for such a system is shown in Fig. 5, where the inbuilt FPGA processor of the OPAL-RT is interlinked with the target PC. The host PC is responsible to execute any command for the OPAL-RT through the compatible RT-LAB software. Moreover, the complete system runs in a hardware synchronization mode with the physical clock time, and also it offers the electrical system and its controller to run with a wide range of sampling time. Therefore, the similar performance

TABLE II
PARAMETERS USED TO DEVELOP THE P.U. GRID-TIED VSC SYSTEM

Parameter	Value	Parameter	Value	Parameter	Value
Rated Power (S_b)	1200 MVA	dc-line inductance (l)	0.5 p.u.	Grid impedance (R_g, L_g)	0.01, 0.2 p.u.
RMS AC voltage	220 kV	Filter resistance (R)	0.003 p.u.	Grid voltage (v_g)	1 p.u.
Angular Frequency (ω_b)	2*π*50 rad/S	Filter inductance (L)	0.08 p.u.	Input voltage (v_{in})	1 p.u.
dc-line resistance (r)	0.007 p.u.	Filter capacitance (C)	0.074 p.u.	Initial value of i_{dr}	-0.8 p.u.

of the RT-LAB model as that of the real-dynamic physical model can obviously be expected. In order to successfully run a model with the GPS time stamping, the RT-LAB in the host PC should follow the commands build, load (with hardware synchronization mode), and execute. In line with this, all the desired signals of the proposed system are collected at the analog-out pins of the OPAL-RT and are captured with the YOKOGAWA scope-coder.

In line with the simulation analysis, the parameters of the PI-controllers employed in the current control loop is firstly tuned for the best value by modulus optimum method (K_p = 1.27, K_i = 14.25), then after MP-RNN with two inputs and two outputs is trained with the same control parameters. Fig. 6 shows some of the key output findings of the considered system under a similar test case as performed for the simulation study. The dc-link voltage oscillation produced under this test case is minimal which can be verified from Fig. 6(a), where the d-axis reference current and actual current wave-shape are also presented to incorporate the dynamic change. Moreover, the proposed controller forces the dc-link current to get settled at the steady-state quickly and with a less oscillatory magnitude as shown in Fig. 6(b). It can also be noticed that the output voltage (a-axis) presented in Fig. 6(c) is not much influenced by the change in d-axis reference current, but the output current magnitude changes accordingly without producing any noise in the shape. In all the above findings, the d-axis component of inverter current (i_{id}) along with its reference component (i_{dr}) is presented, where the accurate tracking of i_{id} is evident.

V. CONCLUSIONS

An MP-RNN based current controller is proposed in this work to tackle the high voltage oscillations produced in a grid-tied VSC system due to the possible LC-resonance and sudden change in reference current/power demand. The ANN structure is further trained by the Levenberg-Marquardt based backpropagation algorithm to obtain the best solution for different disturbance condition. One suitable cost function is defined with three stopping criteria for the successful training process of MP-RNN. The effective workability of the developmental controller over the traditional vector control is validated through the simulation analysis under a large and continuous disturbance conditions. The simulation results clearly demonstrate the superiority of the proposed control in terms of better dynamic performance in damping the oscillation introduced by the dc-link dynamics of the VSC. To further verify the real-time applicability and to cope-up with the simulation study, real-time simulation results of the proposed controller in the OPAL-RT platform are also provided, where the response of the proposed controller to the random disturbances is commendable.

REFERENCES

[1] W. Xiao, H. H. Zeineldin, and P. Zhang, "Statistic and parallel testing procedure for evaluating maximum power point tracking algorithms of photovoltaic power systems," *IEEE J. Photovolt.*, vol. 3, no. 3, pp. 1062–1069, 2013.

[2] A. Blakers, M. Stocks, B. Lu, C. Cheng, and R. Stocks, "Pathway to 100% Renewable Electricity," *IEEE J. Photovolt.*, vol. 9, no. 6, pp. 1828–1833, 2019.

[3] J. Rocabert, A. Luna, F. Blaabjerg, and P. RodrÃguez, "Control of power converters in ac microgrids," *IEEE Trans. Power Electron.*, vol. 27, no. 11, pp. 4734–4749, 2012.

[4] R. K. Agarwal, I. Hussain, and B. Singh, "Application of lms-based nn structure for power quality enhancement in a distribution network under abnormal conditions," *IEEE Trans. Neural Netw. Learn. Syst.*, vol. 29, no. 5, pp. 1598–1607, 2018.

[5] T. Dragicevic and M. Novak, "Weighting factor design in model predictive control of power electronic converters: An artificial neural network approach," *IEEE Trans. Ind. Electron.*, vol. 66, no. 11, pp. 8870–8880, 2019.

[6] M. Amin and M. Molinas, "Understanding the origin of oscillatory phenomena observed between wind farms and hvdc systems," *IEEE J. Emerg. Sel. Topics Power Electron.*, vol. 5, no. 1, pp. 378–392, 2017.

[7] M. Amin and M. Molinas, "A gray-box method for stability and controller parameter estimation in hvdc-connected wind farms based on nonparametric impedance," *IEEE Trans. Ind. Electron.*, vol. 66, no. 3, pp. 1872–1882, 2019.

[8] F. U. Nazir, N. Kumar, B. C. Pal, B. Singh, and B. K. Panigrahi, "Enhanced sogi controller for weak grid integrated solar pv system," *IEEE Trans. Energy Convers.*, vol. 35, no. 3, pp. 1208–1217, 2020.

[9] B. Singh, D. T. Shahani, and A. K. Verma, "Neural network controlled grid interfaced solar photovoltaic power generation," *IET Power Electron.*, vol. 7, no. 3, pp. 614–626, 2014.

[10] R. K. Agarwal, I. Hussain, and B. Singh, "Lmf-based control algorithm for single stage three-phase grid integrated solar pv system," *IEEE Trans. Sustain. Energy*, vol. 7, no. 4, pp. 1379–1387, 2016.

[11] H. C. S. E. De Aldaco and J. A. Alquicira, "Metaheuristic optimization methods applied to power converters: A review," *IEEE Trans. Power Electron.*, vol. 30, no. 12, pp. 6791–6803, 2015.

[12] B. K. Bose, "Artificial intelligence techniques: How can it solve problems in power electronics?: An advancing frontier," *IEEE Power Electron. Mag.*, vol. 7, no. 4, pp. 19–27, 2020.

[13] N. Kumar, I. Hussain, B. Singh, and B. K. Panigrahi, "Implementation of multilayer fifth-order generalized integrator-based adaptive control for grid-tied solar pv energy conversion system," *IEEE Trans. Ind. Informat.*, vol. 14, no. 7, pp. 2857–2868, 2018.

[14] W. Cao, K. Liu, M. Wu, S. Xu, and J. Zhao, "An improved current control strategy based on particle swarm optimization and steady-state error correction for sapf," *IEEE Trans. Ind. Appl.*, vol. 55, no. 4, pp. 4268–4274, 2019.

[15] Y. Sun, S. Li, B. Lin, X. Fu, M. Ramezani, and I. Jaithwa, "Artificial neural network for control and grid integration of residential solar photovoltaic systems," *IEEE Trans. Sustain. Energy*, vol. 8, no. 4, pp. 1484–1495, 2017.

[16] M. Babaie, M. Sharifzadeh, and K. Al-Haddad, "Adaptive ann based single pi controller for nine-level puc inverter," in *2019 IEEE Electrical Power and Energy Conference (EPEC)*, 2019, pp. 1–6.